

**THERMAL MOONQUAKES: IMPLICATIONS FOR SURFACE PROPERTIES.** R. C. Weber,<sup>1</sup> J.-L. Dimech<sup>1</sup>, D. Phillips<sup>2</sup>, J. Molaro<sup>3</sup>, N. C. Schmerr<sup>4</sup>, and C. Fassett.<sup>1</sup> <sup>1</sup>NASA Marshall Space Flight Center (renee.c-weber@nasa.gov); <sup>2</sup>Univ. of Alabama, Huntsville; <sup>3</sup>Planetary Science Institute; <sup>4</sup>Univ. of Maryland, College Park.

**Introduction:** Apollo 17's Lunar Seismic Profiling Experiment's (LSPE) primary objective was to constrain the near-surface velocity structure at the landing site using active sources detected by a 100 m-wide triangular geophone array [1,2]. The experiment was later operated in "listening mode," and early studies of these data revealed the presence of thermal moonquakes – short-duration seismic events associated with terminator crossings [3,4]. However, the full data set has never been systematically analyzed for its natural seismic signal content.

Lost LSPE data have been newly restored by the efforts of the ALSEP Data Recovery Focus Group [5]. In this study, we analyze 8 months of continuous LSPE data using an automated seismic event detection technique that was previously successfully applied to the Apollo 16 Passive Seismic Experiment data [6]. We detected ~50,000 thermal moonquakes from three distinct event templates, representing impulsive, intermediate, and emergent onset of seismic energy [7]. Impulsive events mostly occur at sunrise, while emergent events mostly occur at sunset. By applying an iterative event location algorithm to a pilot study of 40 events, we investigate whether thermal moonquakes represent cracking or slumping in nearby surface rocks and regolith. We also perform 3D modeling of the lunar surface to explore the relative contribution of the lander, known rocks, and surrounding topography to the thermal state of the regolith in the vicinity of the Apollo 17 landing site over the course of the lunar diurnal cycle.

**Locations:** Early work used signal amplitudes to locate thermal events detected by LSPE [4]. Comparison of source locations with topographic features near the LSPE array (Apollo 17 PanCam images) showed that thermal moonquakes are associated to some degree with large rocks and to a larger degree with craters, concluding that thermal moonquakes are the seismic expression of a phenomenon that is actively degrading slopes on the lunar surface (thermal movement of the regolith). This process could be actively contributing to crater degradation. However, event locations from that study were only accurate to ~50m, approximately equal to the array spacing between geophones.

*Application of a modern location algorithm.* In our pilot study, we first applied a simple iterative event location algorithm that has been demonstrated to be effective for small-aperture arrays [8]. The method makes the simplifying assumption that waves travel in a 1-D constant velocity model in a direct path along the surface,

but can be expanded to layered media. We input initial guesses for the seismic velocity and event origin time, and grid search over those parameters such that the misfit between observed and calculated arrivals is minimized. Example results are shown in Figure 1.

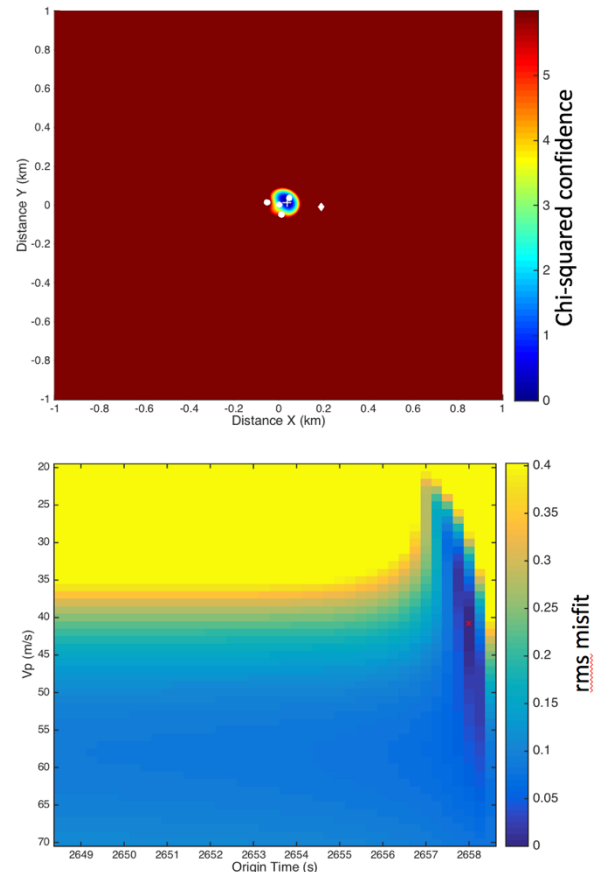


**Figure 1:** (top) Best-fit location for a search over a 1-km square grid centered on the geophone array. Station locations (circles) and the Lunar Module location (diamond) are shown. (bottom) Misfit map in velocity/origin time space. The minimum misfit is marked with a red 'x.' Note that the low velocity is due to the large spread in observed arrivals. Further refinement of this method will account for the maximum distance/travel time difference between stations, forcing the solution away from these unrealistically low values.

The best-fit locations for all events in the pilot study are shown in Figure 2. Arrival pick uncertainty has not yet been mapped to location uncertainty; we chose a misfit of 0.5 seconds to contour location uncertainties.

Locations outside the array appear well constrained in distance but not in azimuth, which is expected due to the tight array geometry.

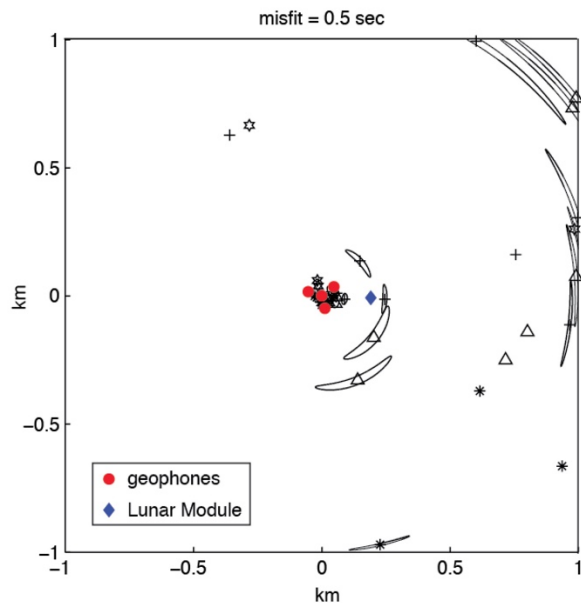


**Figure 2:** Locations for all 40 events in the pilot study (open symbols), with 0.5s rms misfit contours. Some events do not have contours because the misfit never reached the 0.5s threshold (indicating they are the most poorly constrained). Red circles are geophone locations; blue diamond is the Lunar Module.

*Location interpretation:* The pilot study demonstrated that thermal moonquake arrival times can be used to improve precision of recovered locations over previous studies, especially for events located within the array. While there is a clear temporal pattern with impulsive events at sunrise and emergent events at sunset, there is no obvious spatial pattern which would help discriminate between these two event types – and thus no immediate clues as to their causal mechanism. However, the pilot study sample size is small, and we plan to follow up with an analysis using a larger number of events before ruling out the possibility of spatial patterns. Locations are shown plotted over LROC imagery of the landing site in Figure 3. The distribution of recovered locations suggests diffuse events throughout the lunar regolith, but because of large separations in the delay times between events, it is not possible to rule out contributions from regional rocks and boulders until pick uncertainty is properly included in the analysis.

*Thermal modeling:* Recent 3D finite-element thermal stress modeling has shown that the stress response in lunar boulders varies as a function of boulder size and diurnal cycle [9]. During sunrise, stresses (and resultant

cracking) occur in the boulders' interiors associated with large-scale temperature gradients developed due to overnight cooling. During sunset, stresses occur at the boulders' exteriors due to the cooling and contraction of the surface. This process may be consistent with thermal moonquake occurrence, since we observe differing waveform types at sunrise vs. sunset. While our initial thermal moonquake locations are not coincident with any detectable rocks or boulders, we note that LROC can only resolve boulders down to ~1m scale, while thermally-induced rock breakdown occurs at scales down to ~30cm. Many small rocks are observed in the Apollo 17 surface panoramas, suggesting that thermal moonquakes may contribute to regolith production in addition to crater degradation.

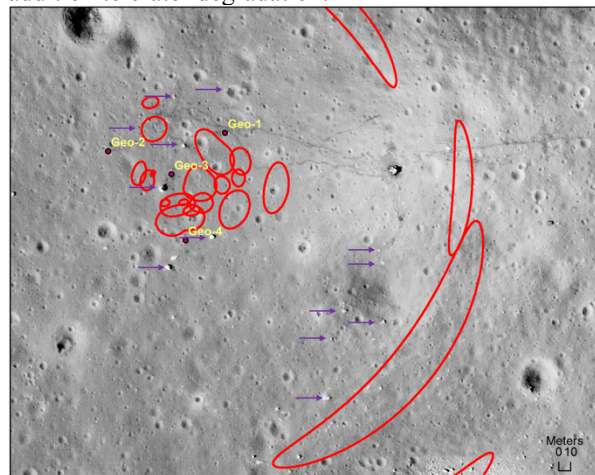


**Figure 3:** LROC image of the Apollo 17 landing site, zoomed into the vicinity of the geophone array. Red contours are thermal moonquake locations. Purple arrows indicate the locations of rocks and boulders.

**References:** [1] Heffels, A.; Knapmeyer, M.; Oberst, J.; Haase, I. (2017) *PSS 135*, 43–54. [2] Sollberger, D.; Schmelzbach, C.; Robertsson, J. O. A.; Greenhalgh, S. A.; Nakamura, Y.; Khan, A. (2016) *GRL 43*, 10,078 – 10,087. [3] Duennebier, F. and Sutton, G. H. (1974) *JGR 79*, 4351 – 4363. [4] Duennebier, F. (1976) *Proc. Lunar Sci. Conf. 7<sup>th</sup>*, 1073 – 1086. [5] Nagihara, S.; Nakamura, Y.; Williams, D. R.; Taylor, P. T.; McLaughlin, S. A.; Hills, H. K.; Kiefer, W. S.; Weber, R. C.; Dimech, J.-L.; Phillips, D.; Nunn, C.; Schmidt, G. K. (2017) *LEAG Abstract #5017*[6] Knapmeyer-Endrun, B. and Hammer, C. (2015) *JGR 120*, 1620 – 1645. [7] Dimech, J.-L.; Knapmeyer-Endrun, B.; Phillips, D.; Weber, R. C. (2017) *Results in Physics 7*, 4457 – 4458. [8] Schmerr, N. C.; Garnero, E.; Hurford, T.; Lekic, V.; Panning, M.; Rhoden, A.; Yu, H. (2017) *LPSC Abstract #1254*. [9] Molaro, J.; Byrne, S.; Le, J.-L. (2017) *Icarus 294*, 247 – 261.